Published in final edited form as:
Development. 2008 January ; 135(2): 217–225.

The serine protease Corin is a novel modifier of the agouti pathway

David Enshell-Seijffers, **Catherine Lindon**, and **Bruce A. Morgan***
Cutaneous Biology Research Center, Harvard Medical School and Massachusetts General Hospital, 149 13th St. Charlestown, MA, USA 02129.

Summary

The hair follicle is a model system for studying epithelial-mesenchymal interactions during organogenesis. While analysis of the epithelial contribution to these interactions has progressed rapidly, the lack of tools to manipulate gene expression in the mesenchymal component, the dermal papilla, has hampered progress towards understanding the contribution of these cells. In this work, *Corin* was identified in a screen to detect genes specifically expressed in the dermal papilla. It is expressed in the dermal papilla of all pelage hair follicle types from the earliest stages of their formation, but is not expressed elsewhere in the skin. Mutation of the *Corin* gene reveals that it is not required for morphogenesis of the hair follicle. However, analysis of the "dirty blonde" phenotype of these mice reveals that the trans-membrane protease encoded by *Corin* plays a critical role in specifying coat color and acts downstream of *agouti* gene expression as a suppressor of the agouti pathway.

Keywords

Corin; dermal papilla; agouti; pigmentation

Introduction

The hair follicle is an important model system for the study of organogenesis in part because of the attributes that make it amenable to study during follicular neogenesis in the embryo and newborn animal and in part because the lower portion of the hair follicle is regenerated from comparatively well-defined keratinocyte stem cells in the adult. In both neogenesis and regeneration, inductive signaling between epithelium and mesenchyme directs morphogenesis of the follicle. In the embryo, pluri-potent keratinocytes in the basal epidermis initiate follicular development by forming a thickened epidermal placode in response to inductive signals from the dermis. Signals from the placode recruit dermal cells to aggregate beneath it and form the dermal condensation, which in turn acquires additional inductive properties. These include signals required for the growth of the placodal keratinocytes and their invagination to form the hair peg that extends into the dermis. The dermal condensate further differentiates into the dermal papilla (DP) which is engulfed by the extending hair peg and comes to lie in the center of the hair bulb at the base of the mature follicle.

During the active growth phase, the mature hair follicle is composed primarily of keratinocytes arranged in concentric layers of differentiated cell types that comprise the hair shaft (HS), inner root sheath (IRS) and outer root sheath (ORS). Growth of the hair occurs as proliferating cells in the hair matrix at the base of the follicle generate additional constituents of the inner layers of the follicle that are organized into the IRS and HS and extruded through the ORS towards the surface of the skin. The DP plays a central role in this process. The keratinocytes abutting

*Author for correspondence: bruce.morgan@cbrc2.mgh.harvard.edu, phone: 617-726-4446, Fax: 617-726-4453.

the DP act as stem cells of the hair bulb, undergoing asymmetric divisions to generate transit amplifying (TA) progeny that then undergo a few divisions before terminally differentiating (Legue and Nicolas, 2005). Ablation and grafting studies have demonstrated that the DP is required to maintain the growth of the hair follicle and suggest that it plays an instructive role in driving morphogenesis of the hair (Jahoda et al., 2001; Oliver and Jahoda, 1988).

This period of sustained hair growth lasts for a few weeks in the mouse. At the end of this growth or anagen phase, proliferation in the hair bulb ceases. During the degeneration or catagen phase, the matrix cells either terminally differentiate or apoptose, and the basal end of the hair shaft becomes anchored in the upper follicle. The outer root sheath from the lower 2/3 of the follicle degenerates and the DP is drawn to the base of the permanent portion of the follicle. A quiescent or telogen phase ensues that may last from a few days during the first hair cycle to many weeks in mature animals. At the end of the telogen phase, keratinocyte stem cells resident in the bulge region of the permanent follicle are activated and regenerate the lower portions of the anagen follicle (Morris et al., 2004). It is thought that the DP plays a central role in the activation of these keratinocytes and the subsequent guidance of their proliferation and differentiation to regenerate the follicle, although the nature of that role remains to be empirically defined (Sun et al., 1991).

In addition to its functions in follicle morphogenesis and cycling, the DP also regulates pigmentation of the hair. Pigment is synthesized by melanocytes resident in the hair bulb and deposited in the keratinocytes of the hair medulla and cortex. Pigment production in melanocytes is regulated in part by the activity of the Mc1r receptor expressed on their surface. When this receptor is active, the black pigment eumelanin is produced and deposited in the hair shaft. Mc1r has a basal level of constitutive activity in the absence of its agonists melanocortins that is further stimulated by the binding of these ligands (Barsh, 1999; Smart and Low, 2003). While the DP is likely to play a role in generating an environment that attracts and maintains melanocytes in the hair bulb (Yoshida et al., 1996), it also regulates hair pigmentation more directly by expressing the agouti signaling protein, hereafter referred to as agouti (Millar et al., 1995). Binding of agouti to Mc1r reduces its activity and results in a shift from the production of eumelanin to the synthesis of pheomelanin, a yellow pigment (Barsh et al., 2000; Chai et al., 2003). *Agouti, (*also known as *non-agouti or ASIP)* is expressed transiently in the DP of the dorsal pelage during the early growth phase of the hair cycle. The resultant provisional switch to pheomelanin deposition generates a sub apical yellow band in the otherwise black hair that defines the agouti coat color. Despite the predominance of black pigment in the hair of agouti mice, the presence of lighter pigment in the hair tip creates the overall appearance of a mottled brown hair coat that provides adaptive coloration in the natural environment. Modest variations in the length of this apical pheomelanin band can dramatically alter coat appearance and are one mechanism by which adaptive changes in coat color can occur (Hoekstra, 2006).

Due in part to the development of mouse strains that allow the manipulation of gene expression in either the embryonic precursors of the epidermis and follicular epithelium (Byrne et al., 1994; Indra et al., 1999), the epidermal placode (Levy et al., 2005), or the stem cells of the adult hair follicle (Ito et al., 2005), significant progress has been made in understanding the genetic mechanisms that direct follicle formation in its keratinocyte constituents. Despite its functions in maintaining the niche for matrix stem cells and in organizing both the morphogenesis and pigmentation of the hair follicle, the molecular genetics of DP formation and function have remained less accessible to study because of a comparative lack of tools to purify these cells or manipulate gene expression in vivo. To address this need, we evaluated genes preferentially expressed in the DP of the hair follicle to identify those whose expression was highly specific to this population. Here we report the identification of *Corin* as a gene specifically expressed in the DP of the hair follicle. Ablation of *Corin* activity in the DP reveals

that it is not required for hair follicle morphogenesis and confirms the *Corin* gene is well suited to serve as a platform for the manipulation of gene expression in the DP in vivo. This analysis also reveals an unexpected function for this transmembrane serine protease in the regulation of hair shaft pigmentation and identifies a novel mechanism by which the DP directs the pattern of pigmentation in the hair shaft.

Materials and Methods

Mice

Using a 129SvJ ES-cell line, 64bp downstream of the ATG in exon1 of *Corin* was replaced by a YFP-Neo cassette. Chimeric mice (A^w/A^w), derived from correctly targeted ES clones, were crossed with C57BL6J (a/a) to generate F0 mice heterozygous for both *Corin* and *agouti* (A^W/a). F0 mice were crossed with FVB (A/A) to generate F1 mice (either A^W/A or A/a). Phenotypic analysis was performed on offspring from matings of F1 *Corin*-heterozygous mice. Qualitatively similar results were obtained when the *Corin* allele was first moved to either FVB, C57BL6J or 129 backgrounds for at least 6 generations.

In-situ hybridization and immunohistochemistry

Non-radioactive in situ hybridization to sections from embryos and dorsal skins were performed with probes corresponding to nts 682-1252 of *Corin* (NM_016869) and nts 126-613 of *Agouti* (NM_015770). Anti-Corin antibodies (1:800) raised in rabbits against (Fig. 2A), were detected with FITC-conjugated secondary antibody (1:250)(Jackson) in the presence of TO-PRO-3 (1:40000).

Hair shaft analysis

The analysis of the length of the subapical yellow band was performed on 6 wild-type and 7 mutant P20 mice. At p20, hairs derived from the first hair cycle are fully grown and the only hairs present in the dorsal pelage. For each mouse, approximately 400 hairs from mid-dorsal pelage were randomly mounted on slides in a thin layer of Gelvatol. Awl hairs represent approximately 10% of the total hair population. Therefore, about 80 awl hairs per mouse were specifically collected for analysis. Two-tailed unpaired t-tests were performed.

Hair shafts were photographed in bright field and in green fluorescent channel at 100X magnification. Lack of black pigment in the hair shaft results in autofluorescence that corresponds with the deposition of yellow pigment. The green channel of the fluorescent image was duplicated in the red channel to generate a yellow color. The modified fluorescent image was overlaid on the bright field image in PhotoShop and reduced to 45% opacity.

Real-time PCR

Mid-dorsal skins from P0-P9 were collected and used to prepare RNA with Trizol solution (Invitrogen). The total RNA was further purified using RNeasy® mini kit (Qiagen) and a DNase I digestion step. Normalized RNA were reverse transcribed using random hexamer primers. Primer pairs (Superarray) for *B-actin* (PPM02945A), *Corin* (PPM41062A), *Agouti* (PPM24722A), *Mc1r* (PPM04903A), *Pomc1* (PPM37114A), *Atrn* (PPM30947A) and *Mgrn1* (PPM02945A) and CYBR Green/Fluroescein PCR Mater Mix were employed with an iCycler (BioRad), MyiQ Single-color Detection system, MyiQ Optical System Software. Differences between samples were quantified based on the ΔΔCt method. The number of mice per genotype (WT/Mut) per stage used in this expression profile was as follows: P0(5/3); P1(9/10); P2 (13/10); P3(8/7); P4(13/9); P5(7/11); P6(5/6); P7(3/4); P8(2/2); P9(4/5). The analysis was performed individually for each mouse and the average values were calculated for each group

of mice. Thus, the standard deviation reflects the variation in gene expression between individual mice in the same group.

Results

Corin is preferentially expressed in DP cells

As an initial step towards identifying genes that might serve as platforms for the study of DP function, a mouse expressing EGFP under the control of a short segment of the human versican promoter was employed (Kishimoto et al., 2000). A population enriched in DP cells was purified from newborn skin on the basis of GFP expression (Shimizu and Morgan, 2004). Gene expression in these cells immediately after isolation was compared with that of cells maintained in culture with the expectation that genes expressed in the DP as a consequence of inductive signaling from the follicular keratinocytes would be preferentially lost from the cultured cell expression profile. Among the genes identified in this way was the *Corin* locus. *Corin* transcripts were readily detected in freshly isolated cells but dropped below the level of detection within 24 hrs in culture (Fig. S1). *Corin* encodes a transmembrane protease that is expressed in the heart and participates in blood pressure regulation by cleaving the prohormone proANP to its active form (Chan et al., 2005; Yan et al., 2000). EST expression profiles and available expression data suggested that *Corin* expression was largely restricted to cardiomyocytes, (see also Yan et al., 1999). This restricted expression profile and the expression of the Corin protein on the surface of the cell made this gene an attractive candidate for further investigation of its expression and function in the skin. Although mice lacking Corin have the altered blood pressure regulation and cardiovascular defects predicted by its role in cleaving ANP, no skin or hair phenotypes were reported in these mice (Chan et al., 2005).

Corin expression in the hair follicle

Hair follicle formation occurs in three waves during embryogenesis that initiate at E14, E16 and between E18 to birth. These waves give rise to follicles that generate distinct hair types. Follicles that give rise to the long, straight guard hairs arise in the first wave, while the intermediate sized awl and smaller zigzag and auchene hair types are thought to arise in the second and third waves respectively. *Corin* expression at the RNA level was examined in embryonic skin and in the dorsal pelage of post-natal animals by in-situ hybridization (Fig. 1). It is first detected in the skin in the nascent dermal condensate at e15 as the first wave of follicles form (Fig. 1A). Its expression persists in the DP throughout the development of these follicles and is also observed in the dermal condensate and DP of the second and third waves of follicles throughout their morphogenesis (Fig. 1B,C). Corin transcripts were not detected elsewhere in the skin at any stage examined. Corin expression persists and remains restricted to the DP throughout the anagen (growth) phase of the hair cycle (Fig. 1D–G and data not shown). Expression is not detected during the catagen (regression) or telogen (resting) phases but returns with the onset of a new anagen phase (data not shown). *Corin* is expressed in a similar pattern in all follicle types of the dorsal pelage.

Corin protein is expressed on the surface of DP cells

Antisera were generated to evaluate Corin protein distribution in the skin. A schematic representation of the inferred protein structure is shown in figure 2A. In addition to the C-terminal protease domain, this type II transmebrane protein has two cysteine rich “frizzled homology” domains, two series of LDLR like repeats and a scavenger receptor conserved region. A segment corresponding to the LDLR repeats 1–5 was expressed in bacteria and used to immunize rabbits. The resultant anti-sera reveal Corin expression in the DP of the hair follicle (Fig. 2B–F). Corin protein levels mirror the expression pattern of *Corin* at the RNA level suggesting that any post-transcriptional events controlling *Corin* activity and function do not include the participation of translational regulation. Furthermore, consistent with the predicted

protein structure, the majority of Corin protein detected remains associated with DP cells (Fig. 2E,F). Although detailed analysis was restricted to dorsal pelage, Corin was also detected in the DP of vibrissae and pelage follicles of the ventral skin.

Corin is not required for hair growth or cycling

A null allele of *Corin* was generated by inserting a YFP-Neo cassette into the first exon of *Corin* that harbors the initiation codon and encodes most of the intracellular N-terminal domain (Fig. 3A). Mice homozygous for this allele (*Corin* −/−) were recovered at expected frequencies and are viable and fertile (Fig. 3B–D). Immunostaining with anti-Corin antibodies confirmed both the absence of detectable Corin protein in these mice and the specificity of the anti-sera used in this study (Fig. 3E–F). In P3 skin, the three waves of follicle formation are represented by follicles in different stages of development. All three stages of hair follicles are present in mutant skin with frequencies similar to wild type, suggesting that hair follicle initiation is normal in homozygous mutants (Figs. 3E–F, S2). Indeed, the hair coat in homozygous mutant animals appears normal with respect to numbers, frequency, structure and growth rate at all stages examined (Figs. 4 and S3). Corin activity is not required for the normal morphogenesis or cycling of the hair follicle.

Corin modifies *agouti* activity

There is, however, a striking difference between the wild-type and mutant pelage. Homozygous mice exhibit a distinctly lighter coat-color that is most pronounced in juveniles but persists through adulthood (Fig. 4A,B). This phenotype is dependent on the presence of a functional allele (*A*) of *agouti*. *Corin* mutants homozygous for a null allele of the *agouti* gene (a/a) are black and indistinguishable from wild type (Fig. 4C), while *Corin* mutants on *A/a* or *A/A* backgrounds are progressively lighter than corresponding mice with a wild-type *Corin* allele (Fig. 4D). The yellow appearance is a result of pheomelanin production and not alteration of the diffractive properties of the hair as tryosinase mutants incapable of synthesizing melanins have white fur irrespective of the presence or absence of Corin (Fig. 4C). Heterozygotes for *Corin* are indistinguishable from wild type on all *agouti* backgrounds tested (data not shown).

To gain more insight on the mechanism underlying the coat-color phenotype, hair shafts were plucked from back skin of wild-type and mutant mice at the end of the first hair cycle. The four types of hair, guards, awls, zigzags and auchenes, differ in the extent of pheomelanin content. Changes in hair type could in principle explain the lighter coat color. However all four types of hair were present in similar frequencies in both wild-type and mutant mice (Fig. S3). *Corin* is not required to specify hair type. The length of the subapical yellow band was analyzed separately for each hair type. Zigzag hairs are the most abundant hair type and have a prominent yellow band. Regardless of *Corin* genotype, all zigzag hairs exhibit a yellow band that is restricted to the apical segment of the hair. In mutant zigzag hairs, the length of the yellow band is increased. Figure 5A shows extreme examples of wild-type and mutant zigzag hairs: in the absence of Corin the yellow band extends for the length of the terminal segment while in wild type it extends less than half of that length. Both the length of the terminal segment and the length of the yellow band vary between different zigzag hairs on the same mouse. To quantify the differences between wild-type and mutant zigzag hairs, the ratio (R) between the length of the yellow band (Y) and the length of the apical segment (Z) was calculated (Fig. 5B). Hairs were scored for the presence or absence of a black tip and assigned to one of three categories: $R \leq 0.5$, $0.5 < R \leq 0.75$, or $0.75 < R \leq 1$ (Fig. 5C–H). This analysis revealed two major differences (see Fig. 5I). First, the basal extension of the yellow band increases substantially in the mutant. The number of zigzag hairs with $R > 0.5$ increases significantly from 33% in wild type to 85% in mice lacking Corin and the category exhibiting $R > 0.75$ increases from essentially absent to 32%. Second, the yellow band is also extended in the apical direction in most hairs. Although virtually all of the wild-type hairs have a terminal black tip, 70% of the

mutant hairs do not (Fig. S4). It is striking that the extension of the yellow band in the apical and basal directions are to some extent independent events. Hairs with the longest yellow bands may nevertheless have a black tip, while hairs in the shortest category may have yellow tips. Despite the breadth of the categories used in this analysis, the pigmentation pattern of a minimum of 85% of the zigzag hairs is altered in the *Corin* mutant.

Similar analysis with some minor modifications was performed for the awl hairs (Fig. 6). The ratio (R) between the length of the yellow band (Y) and the length of the whole hair (A) was calculated (Fig. 6B). In contrast to zigzag hairs, many of the wild-type awl hairs are completely black (R=0 Fig. 6C). Furthermore, regardless of *Corin* genotype, all awl hairs terminate with black tip. Two additional categories were defined: $R \leq 0.25$ and $0.25 < R \leq 0.5$. Representative examples of all three categories are shown in figure 6A. A striking reduction in the frequency of completely black awl hairs from 61% in wild type to 28% in mutant was observed (Fig. 6C). In the absence of Corin, many awl hairs that otherwise would be completely black are transformed to include a subapical yellow band. Furthermore, the percentage of awl hairs with $0.25 < R \leq 0.5$ increases from 7% in wild type to 54% in mutant mice. This increase (47%) exceeds the proportion that could be contributed by awl hairs that normally exhibit a yellow band in wild type (39%) and demonstrates that hairs which would normally lack any discernible agouti activity show pheomelanin deposition over a quarter of their length in the absence of Corin.

A similar elongation of the yellow band as a result of *Corin* ablation was observed in auchene hairs (Fig. S5). As was observed in zigzag hairs, the extension of the pheomelanin band in the apical and basal directions are independent events. Although substantial extension in the basal direction is observed, all mutant auchene hairs end with black tips as observed in wild-type mice. In contrast to zigzags, awls and auchenes, all guard hairs were completely black in both wild-type and mutant mice suggesting that agouti signaling is completely inactive in this type of hair regardless of the presence or absence of Corin (data not shown).

The expression of agouti pathway genes is not altered in *Corin* mutants

The extent of the yellow band is regulated in part by the limited window in which the *agouti* gene is expressed in dorsal skin (Millar et al., 1995; Vrieling et al., 1994), and Corin could in principle modulate signals that impinge on DP cells to regulate the expression of *agouti*. Detailed analysis of agouti expression by real-time PCR during the hair cycle in wild-type mice was performed to define the pattern of *agouti* expression (Fig. 7B). *Agouti* transcript levels are extremely low at p0 but rise rapidly from p1 to p3 and then drop off dramatically to baseline levels by p7. No changes in the levels or timing of *agouti* transcript accumulation are detected in *Corin* mutant mice. This whole skin analysis will preferentially detect the expression of agouti in zigzag hairs that comprise 70% −80% of the dorsal pelage. Therefore, *agouti* expression was also evaluated by in situ hybridization to score expression in guard and awl hair follicles (Fig. 7G). As predicted by the lack of a pheomelanin band in Corin mutant guard hairs, *agouti* expression was not detected in guard hair follicles in either wild-type or mutant mice at any of the time points evaluated, which included p0–p6 (Figs. 7G and S6). However, *agouti* transcripts were readily detected in the DP of some, but not all awl hair follicles from p2. No change in the pattern, timing or apparent levels of *agouti* transcript accumulation was observed in *Corin* −/− skin, and expression in both second and third wave follicles of wild-type and mutant mice was largely extinguished between p6 and p7. Alternatively, Corin might exert its function by modifying the levels of another component in this signaling pathway downstream of agouti. A decrease in Mc1r expression would be expected to render melanocytes more sensitive to agouti inhibition and expand the “agouti band”. *Mc1r* mRNA levels in wild-type mice increase to a peak at P3 as the third wave of hair follicles develop and then declines to a stable baseline level of expression that persists throughout the anagen phase (Fig. 7C). No

change in *Mc1r* expression was detected in the absence of Corin. In addition to directly augmenting Mc1r activity, binding of the agonist α-melanocyte stimulating hormone (α-MSH) to Mc1r competitively inhibits agouti binding (Ollmann et al., 1998). By either mechanism, a decrease in α-MSH levels would be expected to enhance pheomelanin production on an *Agouti* background. Although *Pomc1* (the gene encoding the precursor of α-MSH) is mainly expressed in the brain, it is also expressed at low levels in the skin and in cultured keratinocytes (Slominski and Paus, 1993). Therefore, Corin may act on the environment surrounding the DP to control mRNA levels of *Pomc1*. However, similar low levels of *Pomc1* expression were detected in the skin of wild-type and *Corin* mutant mice throughout anagen (Fig. 7D). In addition to Mc1r, the activity of agouti is dependent on at least two other proteins expressed by the melanocyte, attractin (Atrn) and mahogunin (Mgrn1) (Gunn et al., 1999; He et al., 2003a; He et al., 2003b; Phan et al., 2002). Atrn is a single-pass transmembrane protein that binds agouti, and Mgrn1 is an E3 ubiquitin ligase. While the mechanism by which these proteins modify pigment production remains unknown, the prevailing model is that the simultaneous binding of agouti to Atrn and Mc1r activates Mgrn1 to catalyze ubiquitination events targeting Mc1r for modifications that decrease its activity, possibly by promoting its degradation or internalization (He et al., 2003a). In contrast to *agouti* and *Mc1r* that are predominantly expressed in the DP and the melanocyte respectively, *Atrn* and *Mgrn1* are more widely expressed. The mRNA levels of *Atrn* and *Mgrn1* are stable throughout the anagen phase of the hair cycle and remain unchanged regardless of *Corin* genotype (Fig. 7E,F).

While the lack of Corin does not modify the expression of genes involved in agouti signaling, this analysis does confirm that Corin acts downstream of *agouti* transcript accumulation to modify pigment production. In wild-type mice, follicles expressing agouti in the DP but nevertheless producing eumelanin in the hair bulb are readily detected at p3 and p5 (Fig. 7G and data not shown). In contrast, all follicles expressing *agouti* in the DP at levels detected by in situ hybridization produce pheomelanin in the hair bulb of *Corin* mutant mice (Fig. 7G and data not shown). Thus in the absence of Corin, the expression of *agouti* is sufficient to dictate pheomelanin production, while in the presence of Corin, eumelanin production can occur despite *agouti* mRNA expression.

Discussion

The *Corin* gene as a tool to study the DP

These results reveal that, within the skin, Corin is quite specifically expressed in the DP of hair follicles during the anagen phase of the hair cycle. It is not detected elsewhere in the dermis at any time in development analyzed. This specificity, coupled with a dearth of expression elsewhere other than in cardiomyocytes, makes the *Corin* locus an attractive platform for strategies to manipulate gene expression in the DP. The fact that a functional *Corin* gene is not required for the morphogenesis or cycling of the hair follicle extends the range of such strategies to include knock-ins to this locus. The inability to manipulate gene expression in the DP has been an unfortunate impediment to progress in hair follicle biology and the identification of *Corin* locus as a prime candidate for such approaches is a significant advance.

Corin ablation reveals cryptic agouti expression

These results also demonstrate that *Corin* plays an unexpected role in modifying the balance between eumelanogenesis and pheomelanogenesis. This activity is exerted in concert with the agouti pathway. In the absence of a functional allele of *agouti* there is no discernible effect on pigment production. It is noteworthy that *Corin* expression precedes agouti signaling activity and persists long after the decline of detectable agouti activity, while the phenotypic effects of *Corin* ablation are observed at the start and/or the end of agouti signaling period. As *Corin* expression at the RNA level coincides with protein detection of Corin throughout the anagen

phase of the hair cycle (compare Figs. 1 and 2), translational regulation does not explain the failure of *Corin* to suppress pheomelanogenesis during the entire period of *agouti* expression. Therefore, Corin is only able to effectively counteract agouti activity when the levels of agouti are low, at the peripheries of its bell-shaped curve of expression. This conclusion is supported by the observation that coat color is sensitive to the dosage of *agouti* in the presence of Corin. The length of the pheomelanin band is reduced when *agouti* dosage is halved, presumably because a level of agouti sufficient to overcome Corin-mediated inhibition is only reached closer to the peak period of *agouti* expression. The fact that coat color is also sensitive to the dose of *agouti* in the absence of Corin further demonstrates that agouti levels are limiting for pheomelanin production at the edges of its period of expression.

The ablation of Corin does not alter the timing or level of *agouti* expression, or the expression of other known components of the agouti signaling pathway. Instead, ablation of *Corin* unmasks cryptic agouti activity. This cryptic activity is revealed in *in situ* analysis of *agouti* expression in wild-type skin, where hair follicles containing both *agouti* transcripts in the DP and melanocytes producing eumelanin in the adjacent hair bulb are readily detected. In contrast, the deposition of pheomelanin and the expression of agouti transcripts in the DP are well correlated in *Corin*−/− skin. In the mutant, all DP with detectable *agouti* expression are embedded in hair bulbs that do not exhibit eumelanin synthesis.

The strong correlation between pheomelanin deposition and the detection of *agouti* expression in the DP in the absence of Corin suggests that the DP is the source of physiologically relevant agouti in the regulation of pigment production in the dorsal pelage. This observation further suggests that there are no other functionally significant suppressors of agouti protein activity in the mouse strains studied that contribute to this pattern of pigment deposition, although modifiers of pigment production that act at the level of *agouti* gene expression or independently of *agouti* may also contribute to coat color in these strains. A final corollary to this conclusion is that unlike other hair types, *agouti* expression levels in guard hairs remain below biologically significant levels during the elaboration of hair shafts, which remain black despite the absence of *Corin* activity. This is substantiated by in situ analysis. *Agouti* expression was not detected in the DP of guard hair follicles from P0–P7 under conditions that detected agouti transcripts in awl and zigzag follicles (Figs 7, S6 and data not shown).

Corin acts downstream of *agouti* mRNA expression

These results demonstrate that Corin acts downstream of *agouti* gene transcript accumulation to functionally counteract agouti protein activity. As a protease tethered to the surface of the DP cell, the Corin protein is well positioned to regulate agouti protein activity in several ways. Corin's known substrate is the prohormone Nppa, which when cleaved to its active form contributes to blood pressure regulation by activating the natriuretic peptide pathway (Chan et al., 2005; Wu et al., 2002; Yan et al., 1999; Yan et al., 2000). While we can detect the expression of the *Nppb* and *Nppc* genes that encode related natriuretic peptide precursors in the skin at low levels by PCR, neither these genes nor the signaling receptors Npr1 and Npr2 are detectable in the hair follicle by in situ hybridization under conditions that readily detect the robust expression of *Nppa* and *Nppb* in the heart (data not shown). While we cannot rule out the Npp family as substrates that mediate this effect, alternative mechanisms seem more likely.

Among these, a direct protein-protein interaction with a component of the agouti pathway is a strong possibility. As secreted and transmembrane proteins respectively, agouti, α-MSH (Pomc1), Atrn and Mc1r are all potential targets whose activity could be attenuated (agouti or Atrn) or augmented (Mc1r or α-MSH) by the extra-cellular Corin protease activity. Of these, α-MSH is unlikely to be the target of corin. While Pomc1-null mice have lighter coat-color particularly in the ventral skin, they do not resemble the dramatic effect observed in Corin-deficient mice (Challis et al., 2004; Yaswen et al., 1999). In contrast, the agouti protein is

clearly limiting for the pheomelanin switch in wild-type animals (Miller et al., 1997). The fact that it is secreted from the DP, where Corin levels are high, also makes agouti an attractive candidate for modification by this protease.

The fact that the N-terminal and the C-terminal domains of agouti bind separately and independently to Atrn and Mc1r respectively, and the failure of these two domains to rescue in trans the activity of full-length agouti (He et al., 2001; Ollmann and Barsh, 1999) suggest that binding of agouti to both Atrn and Mc1r forms a ternary complex that is required for agouti signaling. If so, a proteolytic cleavage that physically separates the N-terminal domain from the C-terminal domain would not only render the agouti protein inactive but could also produce competitive antagonists that interfere with agouti binding to both Mc1r and Atrn.

Agouti binding to Mc1r is conformational dependent. Cis and trans conformers with markedly different abilities to compete for Mc1r binding are generated when the C-terminal domain of agouti is synthesized in vitro (McNulty et al., 2005). The fact that agouti protein can assume different conformations with distinct binding capabilities suggests that activity of agouti protein could also be modified by a proteolytic cleavage that promotes a conformational change that reduces or abolishes the affinity of agouti protein for either Mc1r, Atrn or both.

In ventral skin, where agouti levels remain high and promote pheomelanin production through the hair cycle, the majority of agouti protein detected by Western analysis migrates at the position expected of the full-length form (Ollmann and Barsh, 1999). Unfortunately, the low and variable level of agouti protein in dorsal skin, the limited sensitivity of available reagents, and the partial nature of the predicted cleavage events prevent direct assessment of these potential cleavage models in dorsal skin in vivo.

While mechanisms in which corin acts directly on agouti might limit the impact of these observations on human pigmentation, where a postulated role for *agouti* in pigmentation based on linkage analysis remains controversial, they might still have other implications for human health. Ectopic expression of *agouti* in the brain induces obesity by acting on the Mc4r that is normally inhibited by the agouti related protein (Agrp) (Duhl et al., 1994; Manne et al., 1995). Aspects of these two signaling pathways are distinct. First, agouti activity in the brain is dependent on attractin and mahogunin (He et al., 2001) while Agrp activity is not (He et al., 2003a; Ollmann et al., 1997). Second, while the C- and N-terminal domains of agouti must act in concert to inhibit Mc1r activity in vivo, binding of the C-terminal domain of Agrp to its receptor is sufficient for function (Ollmann et al., 1997). Furthermore, the N-terminal domain of Agrp inhibits this function and must be removed by proteolytic cleavage to activate Agrp (Creemers et al., 2006; Jackson et al., 2006). Thus, cleavage between the N- and C- terminal domains are likely to have opposite effects on Agouti and Agrp activity, but other possible proteolytic modifications may have similar effects on both pathways. While *Corin* is not expressed in the CNS (Yan et al., 1999), it is possible that an analogous serine protease modulates the activity of Agrp signaling and thus participates in the process of weight control and energy balance. Whether Corin acts by modifying some component of agouti signaling or by a natriuretic peptide pathway-related mechanism that antagonizes Mc1r responses in melanocytes, these results identify a novel pathway to modulate Mcr activity. Identifying the postulated analogous serine protease in the brain would increase the repertoire of targets for drug development and allow the exploration of new therapeutics against obesity.

Finally, variations in coat color have played a prominent role in discussions of adaptation to the environment and the mechanisms that drive evolution. While a large number of genes contribute to pigmentation either through functions in the generation, migration or maintenance of melanocytes, biosynthesis of eumelanin, or transfer of pigment to recipient cells, comparatively few have been identified that contribute to the pheomelanin/eumelanin switch

that plays such a significant role in coat appearance (Oetting and Bennett, 2007). We note that the *Corin* mutation reproduces the described differences in agouti band length seen in deer mouse populations adapted to lighter colored environments than their woods-dwelling counterparts (Hoekstra, 2006). The observations that levels of agouti signaling are limiting in the switch to pheomelanin production and are effectively regulated by Corin only when agouti activity is marginal identifies a novel route to the phenotypic changes associated with adaptive coloration changes. Loss of function mutations in *Pomc1* cause a similar albeit less dramatic lightening of the dorsal pelage, but also cause obesity and adrenal insufficiency (Krude et al., 1998; Yaswen et al., 1999). Loss of *Corin* function may also incur other fitness costs, as both modest hypertension and cardiac hypertrophy are observed in mutant mice, but these costs are less dramatic (Chan et al., 2005). Furthermore, if pigmentation and cardiovascular regulation employ different substrates, these two processes can be uncoupled by substrate-specificity mutations (Knappe et al., 2004). These attributes, and the lack of other genetic modifiers downstream of agouti expression, suggest that an analysis of the relative contribution of *Corin* mutations to adaptive changes in pigmentation in wild populations will be informative.

In conclusion, these studies identify the transmembrane serine protease Corin as a novel modifier of the agouti signaling pathway that acts downstream of agouti gene expression to suppress agouti protein activity on the pheomelanin/eumelanin switch. The tight restriction of *Corin* expression to the DP during the anagen phase of the hair cycle within the skin, its relative lack of expression elsewhere, and the apparent limitation of its activity to regulation of pigment patterning all suggest that this gene will serve as a useful platform to manipulate gene expression in the DP and thereby broaden its contributions to the understanding of hair follicle biology beyond these important insights into the regulation of coat color.

Supplementary Material

Refer to Web version on PubMed Central for supplementary material.

Acknowledgements

We thank Ying Zheng for genotyping and technical assistance, Hidenao Shimizu for discussions of this work and unpublished data, and the MGH ES core for assistance in generating the mutant mice. This work was supported by a grant to the Cutaneous Biology Research Center from Shiseido, Ltd. and to BAM from the National Institutes of Health (R01AR055256-01).

References

Barsh G. From Agouti to Pomc--100 years of fat blonde mice. Nat Med 1999;5:984–5. [PubMed: 10470066]

Barsh G, Gunn T, He L, Schlossman S, Duke-Cohan J. Biochemical and genetic studies of pigment-type switching. Pigment Cell Res 2000;13(Suppl 8):48–53. [PubMed: 11041357]

Byrne C, Tainsky M, Fuchs E. Programming gene expression in developing epidermis. Development 1994;120:2369–83. [PubMed: 7525178]

Chai BX, Neubig RR, Millhauser GL, Thompson DA, Jackson PJ, Barsh GS, Dickinson CJ, Li JY, Lai YM, Gantz I. Inverse agonist activity of agouti and agouti-related protein. Peptides 2003;24:603–9. [PubMed: 12860205]

Challis BG, Coll AP, Yeo GS, Pinnock SB, Dickson SL, Thresher RR, Dixon J, Zahn D, Rochford JJ, White A, et al. Mice lacking pro-opiomelanocortin are sensitive to high-fat feeding but respond normally to the acute anorectic effects of peptide-YY(3-36). Proc Natl Acad Sci U S A 2004;101:4695–700. [PubMed: 15070780]

Chan JC, Knudson O, Wu F, Morser J, Dole WP, Wu Q. Hypertension in mice lacking the proatrial natriuretic peptide convertase corin. Proc Natl Acad Sci U S A 2005;102:785–90. [PubMed: 15637153]

Creemers JW, Pritchard LE, Gyte A, Le Rouzic P, Meulemans S, Wardlaw SL, Zhu X, Steiner DF, Davies N, Armstrong D, et al. Agouti-related protein is posttranslationally cleaved by proprotein convertase

1 to generate agouti-related protein (AGRP)83-132: interaction between AGRP83-132 and melanocortin receptors cannot be influenced by syndecan-3. Endocrinology 2006;147:1621–31. [PubMed: 16384863]

Duhl DM, Vrieling H, Miller KA, Wolff GL, Barsh GS. Neomorphic agouti mutations in obese yellow mice. Nat Genet 1994;8:59–65. [PubMed: 7987393]

Gunn TM, Miller KA, He L, Hyman RW, Davis RW, Azarani A, Schlossman SF, Duke-Cohan JS, Barsh GS. The mouse mahogany locus encodes a transmembrane form of human attractin. Nature 1999;398:152–6. [PubMed: 10086356]

He L, Eldridge AG, Jackson PK, Gunn TM, Barsh GS. Accessory proteins for melanocortin signaling: attractin and mahogunin. Ann N Y Acad Sci 2003a;994:288–98. [PubMed: 12851328]

He L, Gunn TM, Bouley DM, Lu XY, Watson SJ, Schlossman SF, Duke-Cohan JS, Barsh GS. A biochemical function for attractin in agouti-induced pigmentation and obesity. Nat Genet 2001;27:40–7. [PubMed: 11137996]

He L, Lu XY, Jolly AF, Eldridge AG, Watson SJ, Jackson PK, Barsh GS, Gunn TM. Spongiform degeneration in mahoganoid mutant mice. Science 2003b;299:710–2. [PubMed: 12560552]

Hoekstra HE. Genetics, development and evolution of adaptive pigmentation in vertebrates. Heredity 2006;97:222–34. [PubMed: 16823403]

Indra AK, Warot X, Brocard J, Bornert JM, Xiao JH, Chambon P, Metzger D. Temporally-controlled site-specific mutagenesis in the basal layer of the epidermis: comparison of the recombinase activity of the tamoxifen-inducible Cre-ER(T) and Cre-ER(T2) recombinases. Nucleic Acids Res 1999;27:4324–7. [PubMed: 10536138]

Ito M, Liu Y, Yang Z, Nguyen J, Liang F, Morris RJ, Cotsarelis G. Stem cells in the hair follicle bulge contribute to wound repair but not to homeostasis of the epidermis. Nat Med 2005;11:1351–4. [PubMed: 16288281]

Jackson PJ, Douglas NR, Chai B, Binkley J, Sidow A, Barsh GS, Millhauser GL. Structural and molecular evolutionary analysis of Agouti and Agouti-related proteins. Chem Biol 2006;13:1297–305. [PubMed: 17185225]

Jahoda CA, Oliver RF, Reynolds AJ, Forrester JC, Gillespie JW, Cserhalmi-Friedman PB, Christiano AM, Horne KA. Trans-species hair growth induction by human hair follicle dermal papillae. Exp Dermatol 2001;10:229–37. [PubMed: 11493311]

Kishimoto J, Burgeson RE, Morgan BA. Wnt signaling maintains the hair-inducing activity of the dermal papilla. Genes Dev 2000;14:1181–5. [PubMed: 10817753]

Knappe S, Wu F, Madlansacay MR, Wu Q. Identification of domain structures in the propeptide of corin essential for the processing of proatrial natriuretic peptide. J Biol Chem 2004;279:34464–71. [PubMed: 15192093]

Krude H, Biebermann H, Luck W, Horn R, Brabant G, Gruters A. Severe early-onset obesity, adrenal insufficiency and red hair pigmentation caused by POMC mutations in humans. Nat Genet 1998;19:155–7. [PubMed: 9620771]

Legue E, Nicolas JF. Hair follicle renewal: organization of stem cells in the matrix and the role of stereotyped lineages and behaviors. Development 2005;132:4143–54. [PubMed: 16107474]

Levy V, Lindon C, Harfe BD, Morgan BA. Distinct stem cell populations regenerate the follicle and interfollicular epidermis. Dev Cell 2005;9:855–61. [PubMed: 16326396]

Manne J, Argeson AC, Siracusa LD. Mechanisms for the pleiotropic effects of the agouti gene. Proc Natl Acad Sci U S A 1995;92:4721–4. [PubMed: 7761389]

McNulty JC, Jackson PJ, Thompson DA, Chai B, Gantz I, Barsh GS, Dawson PE, Millhauser GL. Structures of the agouti signaling protein. J Mol Biol 2005;346:1059–70. [PubMed: 15701517]

Millar SE, Miller MW, Stevens ME, Barsh GS. Expression and transgenic studies of the mouse agouti gene provide insight into the mechanisms by which mammalian coat color patterns are generated. Development 1995;121:3223–32. [PubMed: 7588057]

Miller KA, Gunn TM, Carrasquillo MM, Lamoreux ML, Galbraith DB, Barsh GS. Genetic studies of the mouse mutations mahogany and mahoganoid. Genetics 1997;146:1407–15. [PubMed: 9258683]

Morris RJ, Liu Y, Marles L, Yang Z, Trempus C, Li S, Lin JS, Sawicki JA, Cotsarelis G. Capturing and profiling adult hair follicle stem cells. Nat Biotechnol 2004;22:411–7. [PubMed: 15024388]

Oetting, W.; Bennett, D. Mouse Coat Color Genes, vol. 2007 (ed.: International Federation of Pigment Cell Societies. 2007.

Oliver RF, Jahoda CA. Dermal-epidermal interactions. Clin Dermatol 1988;6:74–82. [PubMed: 3063375]

Ollmann MM, Barsh GS. Down-regulation of melanocortin receptor signaling mediated by the amino terminus of Agouti protein in Xenopus melanophores. J Biol Chem 1999;274:15837–46. [PubMed: 10336487]

Ollmann MM, Lamoreux ML, Wilson BD, Barsh GS. Interaction of Agouti protein with the melanocortin 1 receptor in vitro and in vivo. Genes Dev 1998;12:316–30. [PubMed: 9450927]

Ollmann MM, Wilson BD, Yang YK, Kerns JA, Chen Y, Gantz I, Barsh GS. Antagonism of central melanocortin receptors in vitro and in vivo by agouti-related protein. Science 1997;278:135–8. [PubMed: 9311920]

Phan LK, Lin F, LeDuc CA, Chung WK, Leibel RL. The mouse mahoganoid coat color mutation disrupts a novel C3HC4 RING domain protein. J Clin Invest 2002;110:1449–59. [PubMed: 12438443]

Sharov AA, Fessing M, Atoyan R, Sharova TY, Haskell-Luevano C, Weiner L, Funa K, Brissette JL, Gilchrest BA, Botchkarev VA. Bone morphogenetic protein (BMP) signaling controls hair pigmentation by means of cross-talk with the melanocortin receptor-1 pathway. Proc Natl Acad Sci U S A 2005;102:93–8. [PubMed: 15618398]

Shimizu H, Morgan BA. Wnt signaling through the beta-catenin pathway is sufficient to maintain, but not restore, anagen-phase characteristics of dermal papilla cells. J Invest Dermatol 2004;122:239–45. [PubMed: 15009701]

Slominski A, Paus R. Melanogenesis is coupled to murine anagen: toward new concepts for the role of melanocytes and the regulation of melanogenesis in hair growth. J Invest Dermatol 1993;101:90S–97S. [PubMed: 8326158]

Smart JL, Low MJ. Lack of proopiomelanocortin peptides results in obesity and defective adrenal function but normal melanocyte pigmentation in the murine C57BL/6 genetic background. Ann N Y Acad Sci 2003;994:202–10. [PubMed: 12851317]

Sun TT, Cotsarelis G, Lavker RM. Hair follicular stem cells: the bulge-activation hypothesis. J Invest Dermatol 1991;96:77S–78S. [PubMed: 2022884]

Vrieling H, Duhl DM, Millar SE, Miller KA, Barsh GS. Differences in dorsal and ventral pigmentation result from regional expression of the mouse agouti gene. Proc Natl Acad Sci U S A 1994;91:5667–71. [PubMed: 8202545]

Wu F, Yan W, Pan J, Morser J, Wu Q. Processing of pro-atrial natriuretic peptide by corin in cardiac myocytes. J Biol Chem 2002;277:16900–5. [PubMed: 11884416]

Yan W, Sheng N, Seto M, Morser J, Wu Q. Corin, a mosaic transmembrane serine protease encoded by a novel cDNA from human heart. J Biol Chem 1999;274:14926–35. [PubMed: 10329693]

Yan W, Wu F, Morser J, Wu Q. Corin, a transmembrane cardiac serine protease, acts as a pro-atrial natriuretic peptide-converting enzyme. Proc Natl Acad Sci U S A 2000;97:8525–9. [PubMed: 10880574]

Yaswen L, Diehl N, Brennan MB, Hochgeschwender U. Obesity in the mouse model of pro-opiomelanocortin deficiency responds to peripheral melanocortin. Nat Med 1999;5:1066–70. [PubMed: 10470087]

Yoshida H, Hayashi S, Shultz LD, Yamamura K, Nishikawa S, Kunisada T. Neural and skin cell-specific expression pattern conferred by steel factor regulatory sequence in transgenic mice. Dev Dyn 1996;207:222–32. [PubMed: 8906425]

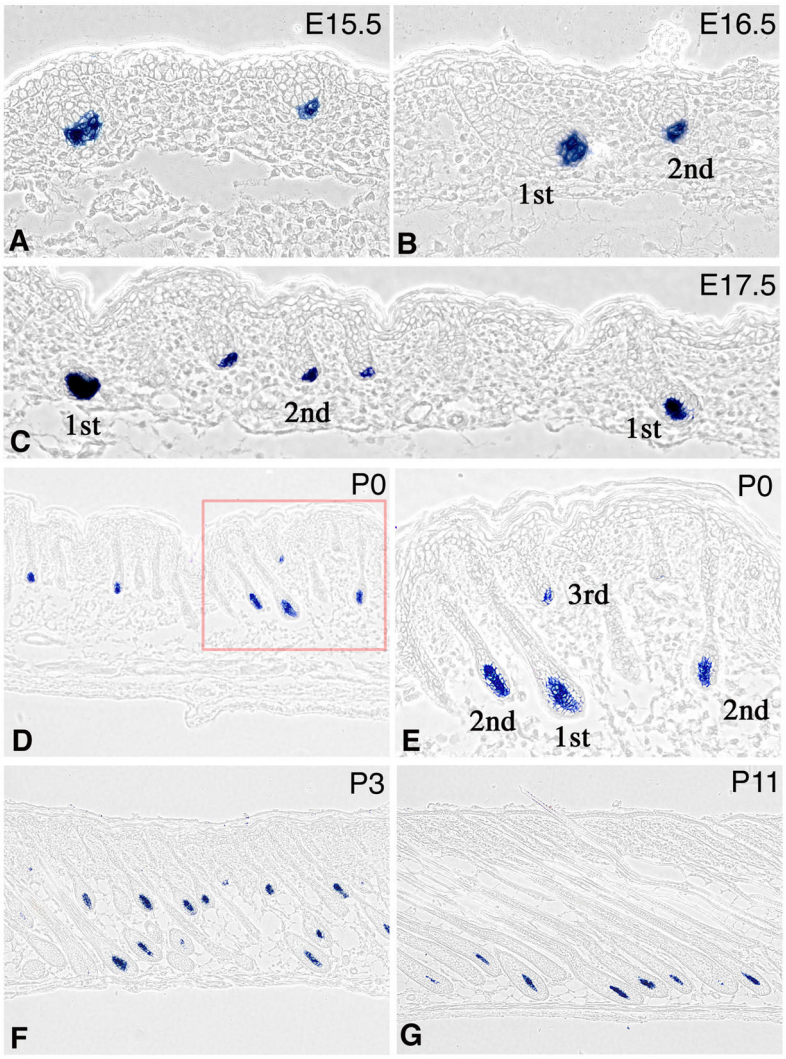

Figure 1. *Corin* expression is confined to the DP

In-situ hybridization to detect *Corin* transcripts (blue) in FVB mice. *Corin* is first detected when the dermal condensate segregates from surrounding dermis during the first (A, E15.5) and second (B, E16.5) waves of follicle formation. Follicles derived from the first, second and third waves of follicle formation are indicated. Throughout the growth phase of the hair cycle, *Corin* transcripts are expressed in the DP and not detected elsewhere in the skin. Samples from E17.5 (C) P0 (D,E), P3 (F) and P11 (G) are shown. The field enclosed by the red square in D is shown in higher magnification in panel E to reveal that *Corin* is expressed throughout the DP and not in the surrounding hair matrix.

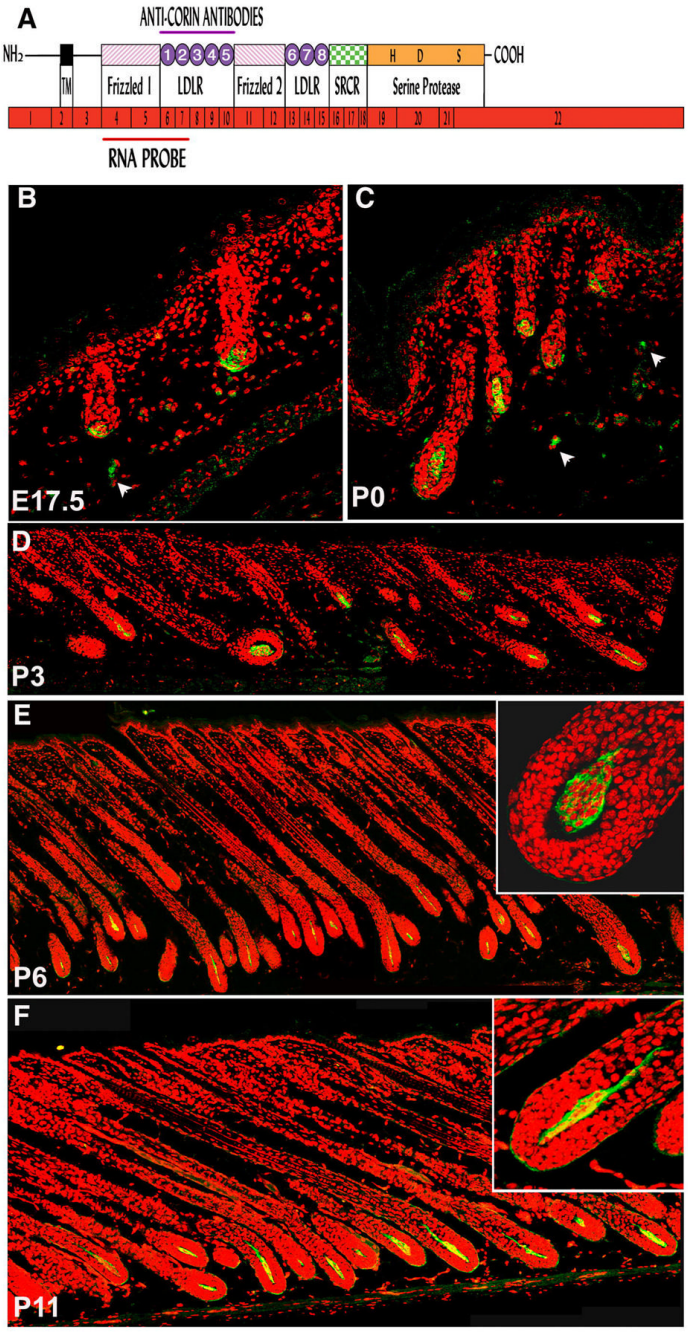

Figure 2. Expression of Corin protein coincides with *Corin* transcript accumulation

(A) Schematic representation of corin mRNA and protein. The mRNA of *Corin* (shown in red) comprises 22 exons encoding a type-II transmembrane serine protease. The single-pass transmembrane domain (TM) of Corin resides in close proximity to the N-terminus, and the large extracellular portion includes two frizzled-like cysteine-rich motifs (designated Frizzled 1 and 2), eight LDL receptor repeats (LDLR 1-8), a macrophage scavenger receptor-like domain (SRCR) and a catalytic domain of trypsin-like serine protease at the C-terminus. The active site residues of the catalytic triad (H, D and S) are shown. The regions corresponding to the RNA probe and the fragment of Corin protein used to immunize rabbits are indicated. (B–F) Immonuhistochemical detection of Corin (green) in DP at E17.5 (B), P0 (C), P3 (D),

P6 (E) and P11 (F). Red stain highlights nuclei. Occasional staining was observed outside the DP (white arrowheads) but this was also detected in controls in which only the secondary antibody was used (data not shown and Fig. S2). In E and F, higher magnification of a bulb region is shown (upper right) to reveal that the majority of the protein is localized at the periphery of DP cells.

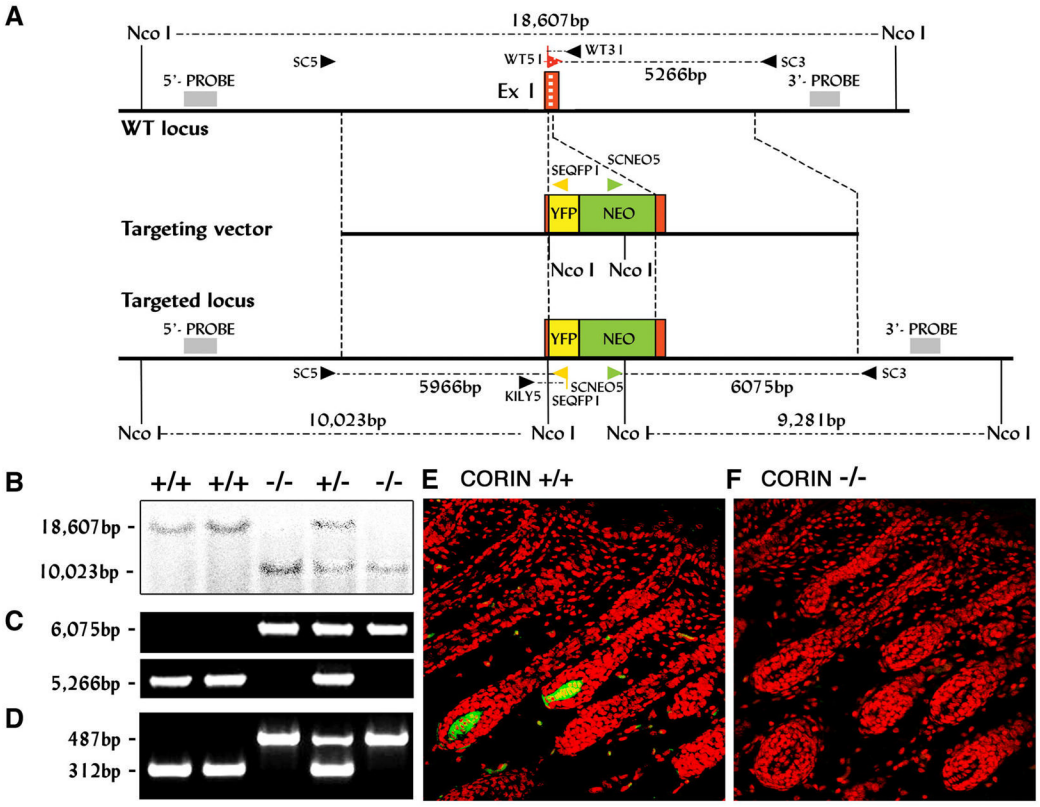

Figure 3. The generation of *Corin* knock-out mice

(A) Gene targeting approach used for corin ablation. A YFP-Neo cassette replaced 64bp downstream of the ATG in exon 1(red box). Primers (arrowheads, see table S1) and expected PCR fragments are indicated. Primer WT51 binds in the deleted-64bp segment and the primers SC3 and SC5 bind outside the targeting construct. The NcoI fragments used for Southern analysis are indicated. The FRT flanked pgkNeo^{R} cassette was oriented in parallel to *Corin* transcription. (B,C,D) Genomic analysis of wild-type, heterozygous and homozygous *Corin* mice. (B) Southern analysis of NcoI-digested genomic DNA. The 5'-probe reveals 18.6kb and 10kb bands from wild-type and mutant alleles respectively. (C) PCR with primers SCNEO5 and SC3 generates a 6075bp band from the targeted allele (upper panel) while WT51 and SC3 generate a 5266bp fragment from wild type. (D) PCR with WT51, WT31, KILY5 and SEQFP1 detects both wild-type (312bp) and mutant (478bp) alleles for routine genotyping. (E,F) Immunostaining of frozen P3 skin-sections from wild-type and mutant mice with anti-Corin antibodies. Corin-green; Nuclei-red.

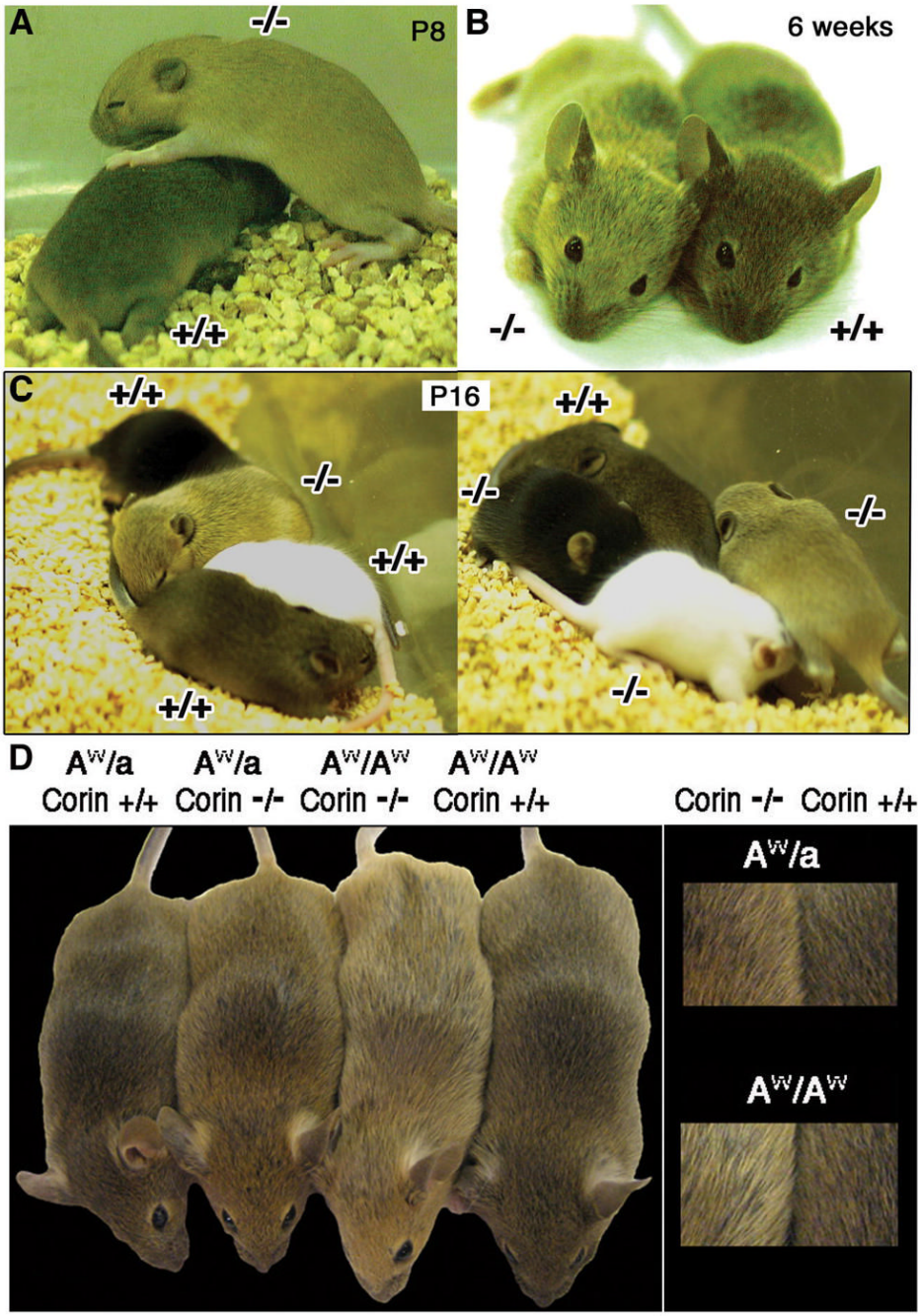

Figure 4. Coat-color phenotype of *Corin* mutants

Mice lacking Corin (−/−) exhibit lighter coat-color than corresponding wild type (+/+) on an *Agouti* background. (A,B) Mice during the first (A) and second (B) hair cycles are shown. (C) Two litters at P16 are shown each containing one *a/a* (black), one *tyrC/tyrC* (white), and two *A/A* with *Corin* genotypes indicated. (D) Pairs of mice homozygous and heterozygous for a functional *agouti* allele and wild-type or mutant for *Corin* are shown with higher magnification views at right. On both *Agouti* genotypes lack of Corin leads to a lighter coat color and in the absence of Corin, A^W/A^W are lighter than A^W/a.

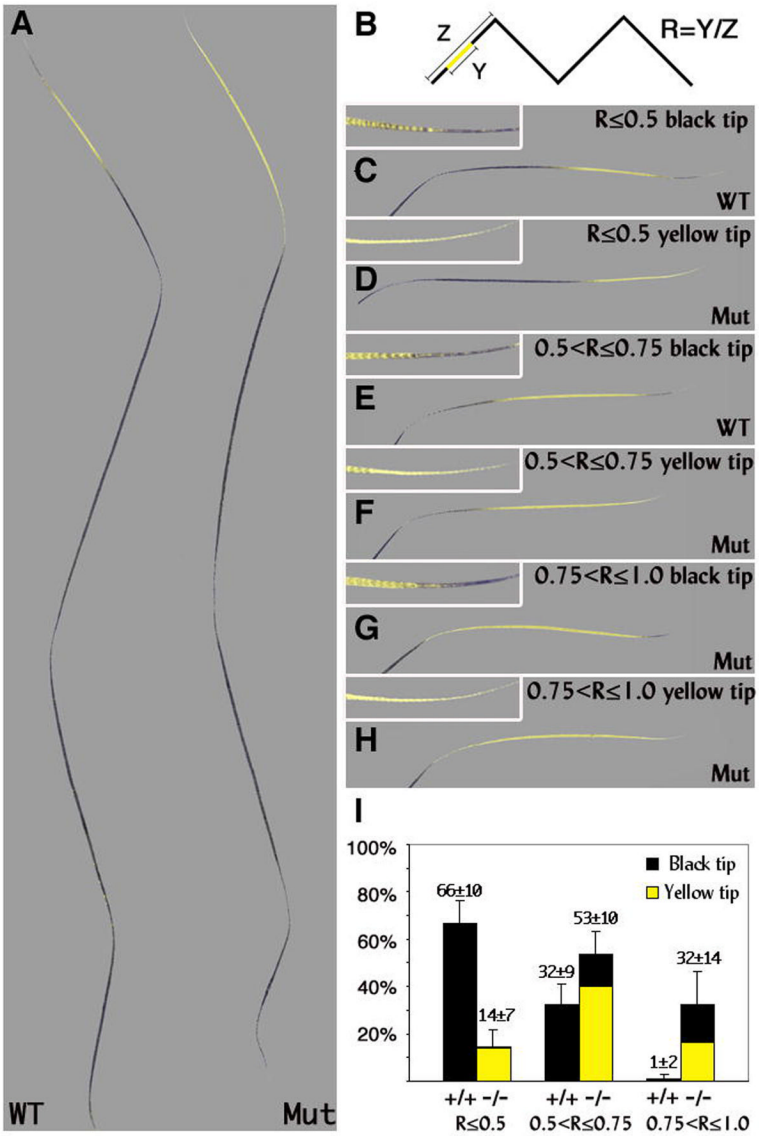

Figure 5. Yellow band extension in *Corin* mutant zigzag hairs

(A) The longest yellow band found in zigzag hairs lacking Corin (Mut) and the shortest subapical yellow band found in wild-type zigzag hairs (WT) are shown. (B) The approach used to quantify the differences between wild-type and mutant zigzag hairs. The ratio (R) between the length of the yellow band (Y) and the length of the apical segment (Z) was scored and assigned to three categories: R≤0.5 (C and D), 0.5<R≤0.75 (E and F), 0.75<R≤1 (G and H). (C–H) The apical segment of representative hairs in these categories is shown. The tip of each hair is shown in higher magnification in the upper left corner. Both the length of the yellow band and the length of the apical segment vary in both wild-type and mutant mice (compare D and F). (I) The distribution of zigzag hairs in wild-type and mutant mice among the above categories is shown including the proportion of black versus yellow tips in each category (black vs. yellow shading respectively). All wild-type zigzag hairs end with a black tip (C,E), while 70% of mutant zigzag hairs exhibit a yellow tip (D,F,H). The hair population of R≤0.5 with black tips that predominates in wild type is almost completely absent in mice lacking Corin.

The category of $0.75<R\leq1$ is essentially unique to mice that lack Corin. The p-values for $R\leq0.5$, $0.5<R\leq0.75$ and $0.75<R\leq1$ are <0.0001, 0.0017 and 0.0002 respectively.

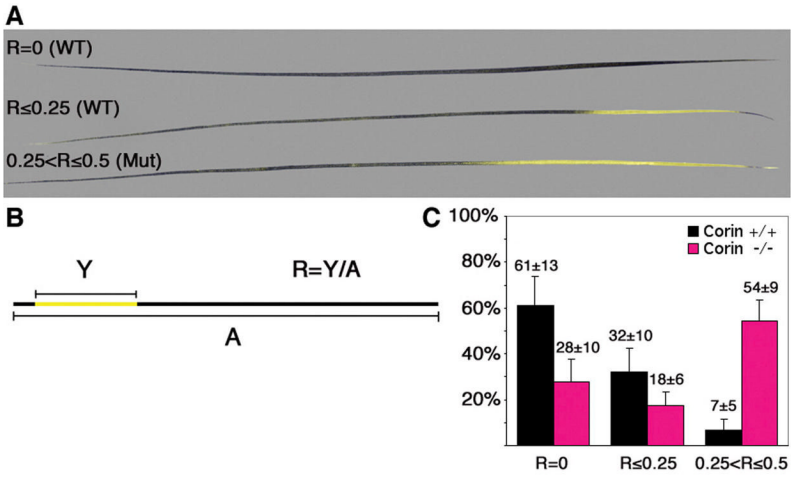

Figure 6. Yellow band extension in *Corin* mutant awl hairs

(A) Representative examples of three categories of awl hairs used in this analysis. In contrast to zigzag hairs, awl hairs may lack a subapical yellow band. (B) The ratio (R) between the length of the yellow band (Y) and the length of the whole hair (A) was calculated and assigned to the categories: R=0, R≤0.25, 0.25<R≤0.5. (C) The distribution of awl hairs among these categories in wild-type (black) and mutant mice (pink). Although a small proportion of 0.25<R≤0.5 is present in wild-type mice, most of these fall close to R=0.25 (data not shown). The p-values for R=0, R≤0.25 and 0.25<R≤0.5 are 0.0002, 0.01 and <0.0001 respectively.

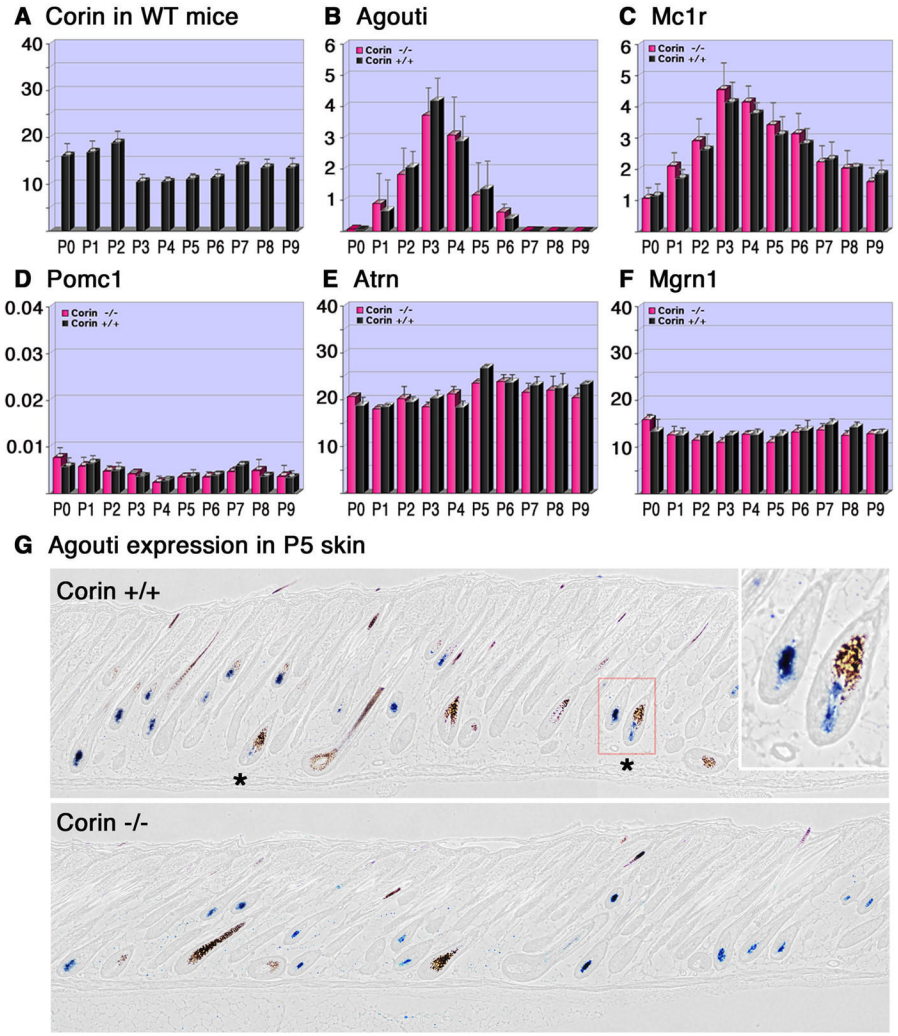

Figure 7. Analysis of the RNA levels of *Corin, agouti, Mc1r, Pomc1, Atrn* and *Mgrn1* throughout the anagen phase of the hair cycle

(A–F) The relative RNA levels determined by Real-time PCR (y-axis) of *Corin* (A), *agouti* (B), *Mc1r* (C), *Pomc1* (D), *Atrn* (E) and *Mgrn1* (F) are shown from birth to P9 (x-axis) for *Corin* +/+ (black) and *Corin* −/− (pink). The RNA levels of all genes tested were normalized to the same units, but different scales employed in A,E,F vs. B,C vs. D. Thus the level of *Atrn* mRNA is about 5 fold higher than the RNA levels of *agouti* at its peak (B and E), while Pomc1 levels are similar to those of *agouti* at its baseline levels from P7 on (B and D). (G) In-situ hybridization of *agouti* in P5 skin. Stars indicate hair follicle bulbs with *agouti* expression in the DP and eumelanin deposition. Note that in the absence of *Corin*, eumelanin deposition has not been detected in the bulb region surrounding *agouti*-expressing DPs. In the right upper corner, higher magnification of the region enclosed by the red square is shown.